Turkish Journal of Electrical Engineering & Computer Sciences

http://journals.tubitak.gov.tr/elektrik/

Research Article

Turk J Elec Eng & Comp Sci
(2021) 29: 1565 – 1581

doi:10.3906/elk-2006-51

In depth study of two solutions for common mode current reduction in six-phase machine drive inverters

Iman ABDOLI, Alireza LAHOOTI ESHKEVARI, Ali MOSALLANEJAD*
Department of Electrical Engineering, Shahid Beheshti University, Tehran, Iran

Received: 09.06.2020 • **Accepted/Published Online:** 26.10.2020 • **Final Version:** 31.05.2021

Abstract: Common mode current (CMC) destroy machine bearings in the long run and increase electromagnetic interference. According to standards, the RMS value of CMC must be lower than 0.3A. Theories show that CMC is originated by applying zero states to the inverter. In this paper, the performance of two solutions in reducing CMC for six-phase machines is investigated. In the first solution, the traditional six-phase inverter is modified by adding two serial power switches on its input terminal. This method is an extended version of a method that has been presented for three-phase inverters, reduces CMC by optimizing the circuit structure. In the second solution, a new space vector modulation (SVM) strategy is proposed, and the inverter topology remains unchanged. In the first method, the modified inverter disconnects from its DC-bus whenever zero vectors are applied, while in the second method, zero vector times are modified. Experimental results evaluate the performance of these two approaches to diminishing the CMC problem. For this purpose, a 380V/5.5kW prototype has been prepared. According to the results, the first solution decreases CMC by 75% below the standard value, and the second method decreases CMC by 45%. Efficiency analysis indicates that the topology modification plan is useful for low-power applications, while modulation improvement can be used for high-power applications due to lower power losses.

Key words: Six-phase, inverter, space vector modulation, common mode current, common mode voltage

1. Introduction

Multiphase electric machines were introduced in the 1960s. Reducing the electromagnetic torque ripple is the main advantage of using multiphase machines so that for an N-phase machine, the lowest order torque ripple value, producing harmonics in the machine phase currents, is of order $(2N \pm 1)$ [1]. In multiphase drive systems, conventional inverters exhibit poor common mode characteristics. This problem occurs due to the common mode impedance paths between the power electronic converter and the machine frame or windings. CMC appears in electric machines due to some stray capacitances between the machine frame/windings and ground. Several sources generate the common mode voltage (CMV) and CMC in variable speed drive systems [2–4]. The RMS value of CMC must be restricted to below 300mA, according to the IEC6100 and VDE0664 standards [5]. Decreasing CMV also reduces CMC. Former research about reducing CMV and CMC in AC machines and grid-connected inverters can be organized into two main categories: the modification of the inverter topology [5–7] and the optimization of modulation methods [2, 8–12]. Optimizing the inverter topology has been done previously for three-phase conventional inverters. For example, a new configuration for three-phase inverters has been introduced by Barter et al. [6]. This inverter includes two additional power switches and two additional

*Correspondence: a_mosallanejad@sbu.ac.ir

power diodes. This topology can decrease the DC-link voltage in the inverter output to $V_{dc}/3$ when zero states are applied. This state occurs whenever upper-side/lower-side switches of the inverter are turned on. By using this technique, the RMS value of CMC is reduced significantly. Rahimi et al. [5] proposed an improved version of the inverter of [6] for grid-connected applications. This inverter is built by using a standard three-phase inverter and two serial power switches; however, those extra power diodes are eliminated. As a result, efficiency is improved significantly in comparison with [6]. This topology reduces the inverter's DC-link voltage to zero whenever the upper-side/lower-side switches of the inverter are turned on. The inverter is disconnected from DC-bus when the inverter's upper-side/lower-side switches are turned on. Lee et al. [13] presents a three-phase inverter with only seven power switches. Although this topology requires one power switch less than the [5], it only disconnects the inverter from the DC-bus in specific switching states. Therefore, it has less impact on CMC. Methods of reducing CMC are also implemented for current-source inverters. For example, a current-source inverter with low CMC has been proposed by Guo [14]. Nevertheless, for six-phase machines, fewer documents have addressed the CMV/CMC problem. Most published articles try to solve this problem by modifying modulation strategies, like those presented in [8, 15–17]. As an instance, Zheng et al. [8] introduced a novel space vector modulation for a six-phase machine. It has classified voltage vectors into 16 groups, and a specific algorithm selects and applies suitable vectors. In [8], the proposed SVM has been implemented on a traditional six-phase inverter. Also, machine windings have been arranged two by two and three single-phase bridge inverters supply each winding. A sawtooth carrier-based PWM has been introduced for asymmetrical six-phase two-level inverter by Liu et al. [15]. Liu et al. [16] has also suggested a novel SPWM with a modified carrier-phase shift.

Studies show the CMV/CMC is reached to the maximum value while applying zero switching vectors [8, 13]. Only two solutions are being considered in this paper to solve this problem. In the first solution, a particular configuration must be designed for the inverter that limits or omits the impact of zero switching events. This solution is an extended version of methods, which are presented for three-phase inverters. In the second solution, the duration of applying zero switching states must be decreased in order to degrade the RMS value of CMC. Thus, in this paper, a simple twelve-sector SVM is presented. Without the need for any complicated algorithm, the SVM must have a symmetrical switching pattern and reduced zero-vector switching time. The second objective is obtained by modifying the dwell-time calculations, which is not considered in other literature. In this paper, the above solutions' performance in reducing CMC for six-phase electric machines is investigated. For the first solution, a conventional six-phase bridge inverter is modified by adding two serial power switches on its input terminal, which is being called hardware optimization. For the second solution, a new SVM strategy is proposed, and the traditional six-phase inverter remains unchanged. Experimental results evaluate the performance of these two approaches in diminishing the explained problem. This article is organized as follows: In Sections 2 and 3, the operating principle of both solutions are being described, respectively. Experimental evaluations are being presented in Section 4. Finally, the proposed methods are compared with other literature. All achievements are summarized in the conclusion.

2. Operating principle of the modified six-phase inverter

There are many parasitic capacitive paths in an induction machine's structure between the windings and rotor, rotor and stator frame, windings and stator frame, and the shaft and bearings, as illustrated in Figure 1a [18]. It is possible to provide an equivalent circuit, as shown in Figure 1b. A model, an equivalent circuit, and the method of calculating its parameters can be found in [19, 20] for further information. It is possible to assume an

equivalent capacitance instead of the equivalent circuit, as presented in Figure 1c, to evaluate an inverter's CMC characteristics without using any sophisticated measurements. As shown in Figure 1c, the inverter operates as an m-phase pulse generator, and the induction machine operates as an m-phase inductive load. An equivalent capacitance is placed between the load neutral-point and the inverter ground. In practice, it is possible to design a test procedure in order to estimate the CMC without a motor. In this test, RL-load is used, and an equivalent capacitor is connected between the load neutral-point and the inverter ground. This capacitance is estimated according to machine parameters like the power rating. CMC is estimated by measuring the passed current through that capacitor. This method has been validated previously by [5] for grid-connected inverters. Figure 2 illustrates the circuit diagram of the proposed inverter topology. It includes 14 power switches, which 12 power switches make a six-phase bridge inverter, and two additional switches place in series with the input source. These power switches are turned on/off according to a particular algorithm. Each inverter leg consists of two series power switches and generates switching-voltage with 60^o phase-shift subject to the adjacent leg. The voltage value across the parasitic capacitor C_p can be obtained based on the stator currents and inductances (L_S). The (1) shows the governing equation on the voltage of parasitic capacitor C_p, where i and j denote the phase label, and z indicates the phase current number, as specified by Figure 2. Besides, the sum of the inverter's output currents is zero in an ideal and balanced condition. Therefore, equation (2) is determined, where 'n' denotes the phase number (Phase A-F). In a nonideal situation, the (2) is not admissible. Therefore, it is reconfigured, as shown by (3).

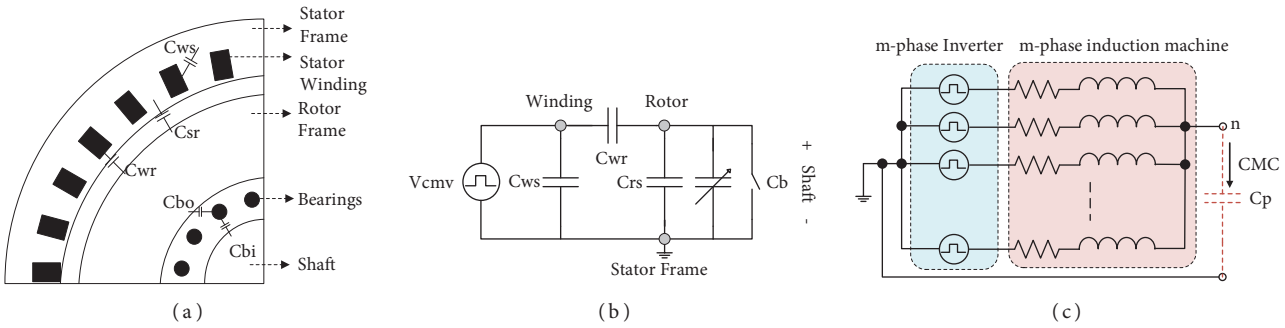

Figure 1. Sources of CMC, (a) distribution of stray capacitances in the induction machine, (b) equivalent circuit of stray capacitances, (c) the location of the equivalent parasitic capacitance.

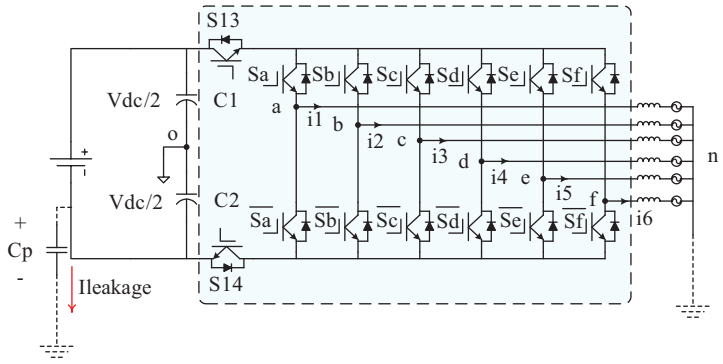

Figure 2. The proposed six-phase bridge inverter.

$$V_{C_P} = -V_{cmij} + \frac{L_s}{2}\frac{di_z}{dt} \tag{1}$$

$$\sum_{n=1}^{n=6} i_n(t) = 0 \tag{2}$$

$$I_{leakage} = -\left(i_1 + i_2 + i_3 + i_4 + i_5 + i_6\right) \tag{3}$$

The summation of possible equations for V_{Cp} obtains a differential equation, as shown by (4).

$$V_{C_P} = -V_{cmvt} - \frac{L_s}{12}\frac{dI_{leakage}}{dt} \tag{4}$$

The common mode voltage (V_{cmv_t}) in a six-phase inverter is determined by (5), where $V_{cm_{ab}}$ to $V_{cm_{fa}}$ represent CMV value between two adjacent phases. Also, the values of $V_{cm_{ab}}$ to $V_{cm_{fa}}$ are derived from (6).

$$V_{cmv_t} = \frac{V_{cm_{ab}} + V_{cm_{bc}} + V_{cm_{cd}} + V_{cm_{de}} + V_{cm_{ef}} + V_{cm_{fa}}}{6} \tag{5}$$

$$V_{cm_{ij}} = \frac{V_{iO} + V_{jO}}{2} \tag{6}$$

Equation (6) shows the values of $V_{cm_{ab}}, V_{cm_{bc}}, \ldots, V_{cm_{fa}}$. The 'i' and 'j' indicate the first and second phase name, respectively. E.g., in $V_{cm_{ab}}$, i=a and j=b. V_{iO} and V_{jO} indicate the voltage of phase 'i' and 'j' respect to the neutral point of the capacitors, as presented in Figure 2. By inserting (6) into (5), (7) is obtained.

$$V_{cmv_t} = \frac{V_{aO} + V_{bO} + V_{cO} + V_{dO} + V_{eO} + V_{fO}}{6} \tag{7}$$

Consequently, the CMV is determined by (7). Sixty-four possible switching states can be substituted in (7) that are listed in Table 1. These states include 10 zero vectors, 37 short vectors, 11 medium vectors, and 6 large switching vectors. The amplitude of short vectors is $V_{dc}/3$, while medium and large vectors have the magnitude of $\sqrt{3}V_{dc}/3$ and $2V_{dc}/3$, respectively. Common mode voltage values produced by each switching event have been given in Table 1. Based on the principle of this inverter, the load is disconnected from the input source during zero vectors by S_{13} and S_{14}. Hence, new CMV values are obtained that have been highlighted in Table 1. Vectors 0 and 63 produce the maximum value of CMV. However, by this method, these vectors cannot produce the CMV. So, the CMC becomes zero. Figure 3 shows an example of a switching event. In this switching interval, the zero vector must be applied to the inverter three times. However, by this method, the inverter is disconnected from DC-bus while applying zero vectors. Thus, the value of CMC becomes zero instead of $V_{dc}/2$. Consequently, the CMC is reduced to zero at those times.

Table 1. List of all switching states and their effect on CMV.

No.	S_f	S_e	S_d	S_c	S_b	S_a	$\overline{V}(t)$	CMV1	CMV in modified bridge
0	0	0	0	0	0	0	0	$-V_{dc}/2$	0
1	0	0	0	0	0	1	$V_{dc}/3$	$-V_{dc}/3$	$-V_{dc}/3$
2	0	0	0	0	1	0	$(V_{dc}/3)\ e^{j\pi/3}$	$-V_{dc}/3$	$-V_{dc}/3$
3	0	0	0	0	1	1	$\left(\sqrt{3}V_{dc}/3\right)\ e^{j\pi/6}$	$-V_{dc}/6$	$-V_{dc}/6$
4	0	0	0	1	0	0	$(V_{dc}/3)\ e^{j2\pi/3}$	$-V_{dc}/3$	$-V_{dc}/3$
5	0	0	0	1	0	1	$(V_{dc}/3)\ e^{j\pi/3}$	$-V_{dc}/6$	$-V_{dc}/6$
6	0	0	0	1	1	0	$\left(\sqrt{3}V_{dc}/3\right)\ e^{j\pi/2}$	$-V_{dc}/6$	$-V_{dc}/6$
7	0	0	0	1	1	1	$(2V_{dc}/3)\ e^{j\pi/3}$	0	0
8	0	0	1	0	0	0	$(V_{dc}/3)\ e^{j\pi}$	$-V_{dc}/3$	$-V_{dc}/3$
9	0	0	1	0	0	1	0	$-V_{dc}/6$	$-V_{dc}/6$
10	0	0	1	0	1	0	$(V_{dc}/3)\ e^{j2\pi/3}$	$-V_{dc}/6$	$-V_{dc}/6$
11	0	0	1	0	1	1	$(V_{dc}/3)\ e^{j\pi/3}$	0	0
12	0	0	1	1	0	0	$\left(\sqrt{3}V_{dc}/3\right)\ e^{j5\pi/6}$	$-V_{dc}/6$	$-V_{dc}/6$
13	0	0	1	1	0	1	$(V_{dc}/3)\ e^{j2\pi/3}$	0	0
14	0	0	1	1	1	0	$(2V_{dc}/3)\ e^{j2\pi/3}$	0	0
15	0	0	1	1	1	1	$\left(\sqrt{3}V_{dc}/3\right)\ e^{j\pi/2}$	$V_{dc}/6$	$V_{dc}/6$
16	0	1	0	0	0	0	$(V_{dc}/3)\ e^{j4\pi/3}$	$-V_{dc}/3$	$-V_{dc}/3$
17	0	1	0	0	0	1	$(V_{dc}/3)\ e^{j5\pi/3}$	$-V_{dc}/6$	$-V_{dc}/6$
18	0	1	0	0	1	0	0	$-V_{dc}/6$	$-V_{dc}/6$
19	0	1	0	0	1	1	$V_{dc}/3$	0	0
20	0	1	0	1	0	0	$(V_{dc}/3)\ e^{j\pi}$	$-V_{dc}/6$	$-V_{dc}/6$
21	0	1	0	1	0	1	0	0	0
22	0	1	0	1	1	0	$(V_{dc}/3)\ e^{j2\pi/3}$	0	0
23	0	1	0	1	1	1	$(V_{dc}/3)\ e^{j\pi/3}$	$V_{dc}/6$	$V_{dc}/6$
24	0	1	1	0	0	0	$\left(\sqrt{3}V_{dc}/3\right)\ e^{j7\pi/6}$	$-V_{dc}/6$	$-V_{dc}/6$
25	0	1	1	0	0	1	$(V_{dc}/3)\ e^{j4\pi/3}$	0	0
26	0	1	1	0	1	0	$(V_{dc}/3)\ e^{j\pi}$	0	0
27	0	1	1	0	1	1	0	$V_{dc}/6$	$V_{dc}/6$
28	0	1	1	1	0	0	$(2V_{dc}/3)\ e^{j\pi}$	0	0
29	0	1	1	1	0	1	$(V_{dc}/3)\ e^{j\pi}$	$V_{dc}/6$	$V_{dc}/6$
30	0	1	1	1	1	0	$\left(\sqrt{3}V_{dc}/3\right)\ e^{j5\pi/6}$	$V_{dc}/6$	$V_{dc}/6$
31	0	1	1	1	1	1	$(V_{dc}/3)\ e^{j2\pi/3}$	$V_{dc}/3$	$V_{dc}/3$
32	1	0	0	0	0	0	$(V_{dc}/3)\ e^{j5\pi/3}$	$-V_{dc}/3$	$-V_{dc}/3$
33	1	0	0	0	0	1	$\left(\sqrt{3}V_{dc}/3\right)\ e^{j11\pi/6}$	$-V_{dc}/6$	$-V_{dc}/6$
34	1	0	0	0	1	0	$V_{dc}/3$	$-V_{dc}/6$	$-V_{dc}/6$
35	1	0	0	0	1	1	$2V_{dc}/3$	0	0
36	1	0	0	1	0	0	0	$-V_{dc}/6$	$-V_{dc}/6$
37	1	0	0	1	0	1	$V_{dc}/3$	0	0

Table 1. (Continued).

No.	S_f	S_e	S_d	S_c	S_b	S_a	$\overline{V}(t)$	CMV1	CMV in modified bridge
38	1	0	0	1	1	0	$(V_{dc}/3)\ e^{j\pi/3}$	0	0
39	1	0	0	1	1	1	$(V_{dc}/3)\ e^{j\pi/6}$	$V_{dc}/6$	$V_{dc}/6$
40	1	0	1	0	0	0	$(V_{dc}/3)\ e^{j4\pi/3}$	$-V_{dc}/6$	$-V_{dc}/6$
41	1	0	1	0	0	1	$(V_{dc}/3)\ e^{j5\pi/3}$	0	0
42	1	0	1	0	1	0	0	0	0
43	1	0	1	0	1	1	$V_{dc}/3$	$V_{dc}/6$	$V_{dc}/6$
44	1	0	1	1	0	0	$(V_{dc}/3)\ e^{j\pi}$	0	0
45	1	0	1	1	0	1	0	$V_{dc}/6$	$V_{dc}/6$
46	1	0	1	1	1	0	$(V_{dc}/3)\ e^{j2\pi/3}$	$V_{dc}/6$	$V_{dc}/6$
47	1	0	1	1	1	1	$(V_{dc}/3)\ e^{j\pi/3}$	$V_{dc}/3$	$V_{dc}/3$
48	1	1	0	0	0	0	$\left(\sqrt{3}V_{dc}/3\right)\ e^{j3\pi/2}$	$-V_{dc}/6$	$-V_{dc}/6$
49	1	1	0	0	0	1	$(2V_{dc}/3)\ e^{j5\pi/3}$	0	0
50	1	1	0	0	1	0	$(V_{dc}/3)\ e^{j5\pi/3}$	0	0
51	1	1	0	0	1	1	$\left(\sqrt{3}V_{dc}/3\right)\ e^{j11\pi/6}$	$V_{dc}/6$	$V_{dc}/6$
52	1	1	0	1	0	0	$(V_{dc}/3)\ e^{j4\pi/3}$	0	0
53	1	1	0	1	0	1	$(V_{dc}/3)\ e^{j5\pi/3}$	$V_{dc}/6$	$V_{dc}/6$
54	1	1	0	1	1	0	0	$V_{dc}/6$	$V_{dc}/6$
55	1	1	0	1	1	1	$V_{dc}/3$	$V_{dc}/3$	$V_{dc}/3$
56	1	1	1	0	0	0	$(2V_{dc}/3)\ e^{j4\pi/3}$	0	0
57	1	1	1	0	0	1	$\left(\sqrt{3}V_{dc}/3\right)\ e^{j3\pi/2}$	$V_{dc}/6$	$V_{dc}/6$
58	1	1	1	0	1	0	$(V_{dc}/3)\ e^{j4\pi/3}$	$V_{dc}/6$	$V_{dc}/6$
59	1	1	1	0	1	1	$(V_{dc}/3)\ e^{j5\pi/3}$	$V_{dc}/3$	$V_{dc}/3$
60	1	1	1	1	0	0	$\left(\sqrt{3}V_{dc}/3\right)\ e^{j7\pi/6}$	$V_{dc}/6$	$V_{dc}/6$
61	1	1	1	1	0	1	$(V_{dc}/3)\ e^{j4\pi/3}$	$V_{dc}/3$	$V_{dc}/3$
62	1	1	1	1	1	0	$(V_{dc}/3)\ e^{j\pi}$	$V_{dc}/3$	$V_{dc}/3$
63	1	1	1	1	1	1	0	$V_{dc}/2$	0

3. Principle of the proposed space vector modulation

Reducing zero switching states' duration and creating a symmetrical switching pattern is highly effective in diminishing common mode. This paper presents a new 12-sector SVM to support the traditional structure. SVM is a straightforward modulation method that provides better THD and a higher modulation index than sinusoidal pulse-width modulation (SPWM). SVM is preferred to other methods because of these features. Studies show that the SVM provides better common mode characteristics than SPWM due to the possibility to optimize zero switching times. In SVM, zero switching times can be divided into several short times in order to achieve a symmetrical switching pattern, better common mode, and current THD. Phase voltages with respect to capacitors neutral point (V_{xo}) are expressed by the following expression, where "x" refers to each phase and

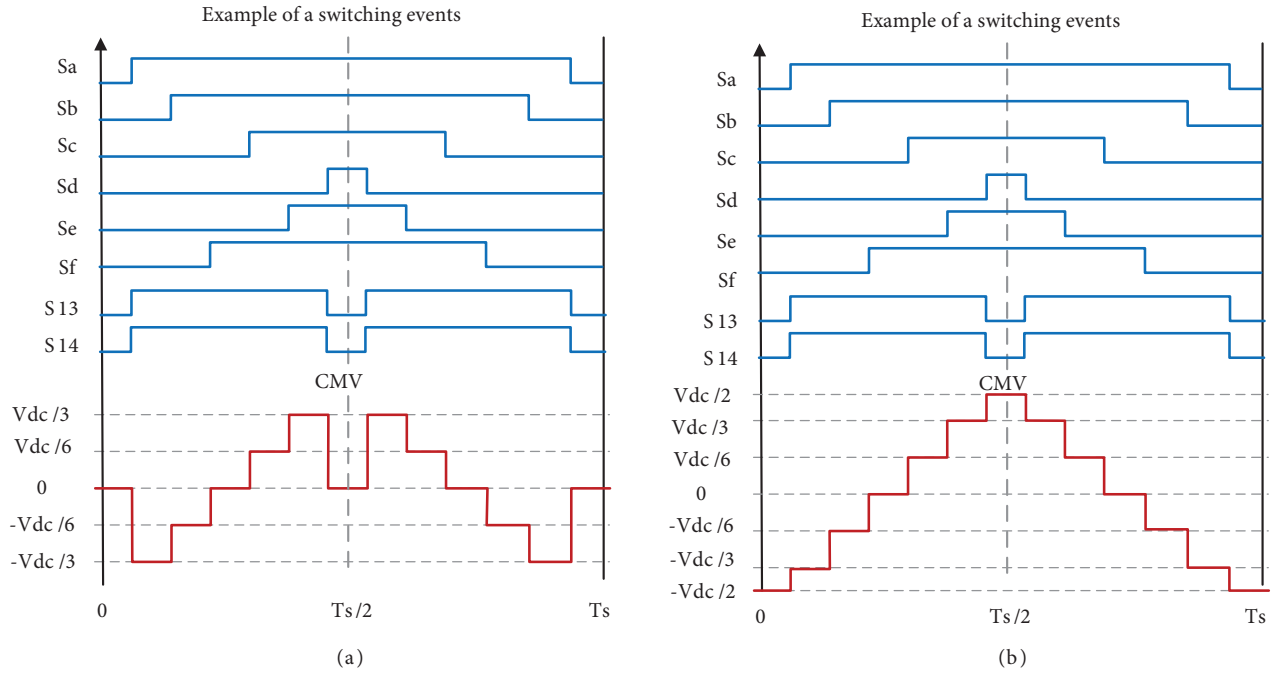

Figure 3. An example of a switching interval, (a) the new switching event, (b) the conventional.

can be "a" to "f". The "S_x" indicates the switching states of the upper switch of each leg.

$$V_{xo} = \begin{cases} +\frac{V_{dc}}{2} & S_x = 1 \ (on) \\ -\frac{V_{dc}}{2} & S_x = 0 \ (off) \end{cases} \tag{8}$$

$$V_{xo} = \left(S_x - \frac{1}{2}\right) V_{dc} \tag{9}$$

$$V_{xn}(t) = V_{xo}(t) + V_{on}(t) \tag{10}$$

The (9) is an algebraic version of (8), in which the phase voltage of inverter with respect to the neutral point of the load (V_{xn}) is obtained by (10), where V_{on} denotes the voltage between the neutral-point and DC-link capacitors. In three-phase systems, it is prevalent to convert reference frames from the three-dimensional frame to the two-dimensional frame for simplicity. In a six-phase system, (11) transforms the reference frame. Therefore, (11) is applied to (10), and (12) is determined.

$$\overline{V} = aV_{an} + a^2V_{bn} + a^3V_{cn} + a^4V_{dn} + a^5V_{en} + a^6V_{fn} \tag{11}$$

$$\overline{V} = \frac{1}{3}\sum_{x=a,j=1}^{x=f,j=6} a^{j-1}V_{xn}(t) \tag{12}$$

In (11) and (12), coefficient 'a' is $e^{j\pi/3}$. The (12) is developed based on the V_{xo} and V_{on} as follows:

$$\overline{V}(t) = \frac{1}{3}\left(\sum_{x=a,j=1}^{x=f,j=6} a^{j-1}\ V_{xo}(t) + \sum_{j=1}^{j=6} a^{j-1}\ V_{on}(t)\right). \tag{13}$$

Since $\left(a + a^2 + a^3 + a^4 + a^5 = 0\right)$, the (14) can be determined as follows:

$$\overline{V}(t) = \frac{1}{3}\sum_{x=a,j=1}^{x=f,j=6} a^{j-1}\ V_{xo}(t). \tag{14}$$

By inserting the (9) into (14), the (15) is derived. It is possible to develop the (15) for the 'm'-phase, as shown by (16). It confirms that the output voltage vector of a six-phase inverter is also rotational, and as a result, SVM can be developed for six-phase inverters.

$$\overline{V}(t) = \frac{V_{dc}}{3}\sum_{x=a,j=1}^{x=f,j=6} a^{j-1}\ S_x \tag{15}$$

$$\overline{V}(t) = \frac{2V_{dc}}{m}\sum_{x=a,j=1}^{j=m} a^{j-1}\ S_x \tag{16}$$

The distribution of voltage vectors in a six-phase inverter has been shown in Figure 4. 64 possible switching states have been presented that performs 10 zero vectors, 37 short vectors, and 11 medium and 6 large switching vectors. The amplitude of short vectors is $V_{dc}/3$, while medium and large vectors have the magnitude of $\sqrt{3}V_{dc}/3$ and $2V_{dc}/3$, respectively. The position of space vectors leads to dividing the hexagon into 12 sectors. So, the theory of the suggested six-phase SVM is better to develop based on twelve sectors. It is assumed that one voltage reference exists, as expressed by (17), where "m_a" denotes the amplitude modulation index.

$$\overline{V}_{ref} = m_a\frac{V_{dc}}{2}e^{j\omega t} \tag{17}$$

$$m_a\frac{V_{dc}}{2}e^{j\omega t} = \frac{T_{11}}{Ts}\left(\frac{2V_{dc}}{6}\ e^{j(i-1)\frac{\pi}{6}}\right) + \frac{T_{12}}{Ts}\left(\frac{4V_{dc}}{6}\ e^{j(i-1)\frac{\pi}{6}}\right) + \frac{T_2'}{Ts}\left(\frac{2\sqrt{3}V_{dc}}{6}\ e^{j(i)\frac{\pi}{6}}\right) \tag{18}$$

The V_{ref} rotates in the space vector diagram of Figure 4 with an angular frequency of ω and the amplitude of $m_aV_{dc}/2$. The value of ωt varies between $(i-1)\frac{\pi}{6}$ and $i\frac{\pi}{6}$, where "i" denotes the sector number (1-12). In each sector, V_{ref} can be rebuilt by its adjacent space vectors. In each sector (from i = 1 to 12), the vector V_{ref} can be rebuilt by a short (for time T_{11}), a medium (for time T_{12}), and large active vectors (for time T_2), so the (18) is determined, where $T_{11} = T_1/2$, $T_{12} = T_1/4$ and $T'_2 = T_2/\sqrt{3}$. T_{11}, T_{12}, and T'_2 are weighting factors and used in order to provide symmetry in inverter output voltage. These coefficients can be used to reduce the zero switching times by increasing the active switching times. By employing (17) and

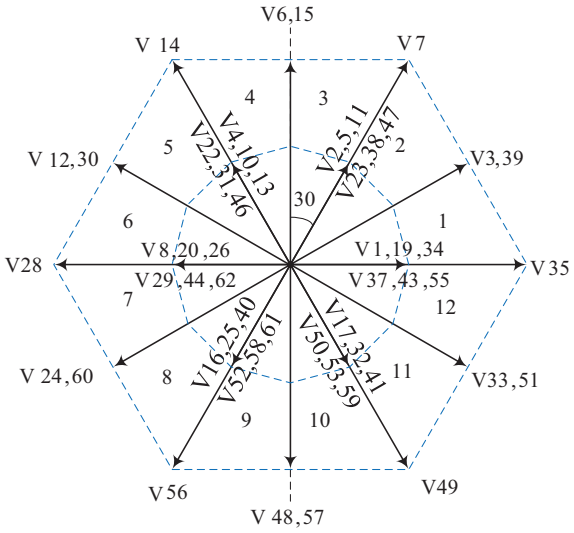

Figure 4. The distribution of voltage vectors in six-phase inverters.

the volt-second principle, the (18) is attained. The (18) is simplified to (19). By solving (19), the (20)–(22) are deduced that provide dwell-times.

$$m_a \frac{V_{dc}}{2} e^{j\omega t} = \frac{T_1}{Ts}\left(\frac{2V_{dc}}{6}\ e^{j(i-1)\frac{\pi}{6}}\right) + \frac{T_2}{Ts}\left(\frac{2V_{dc}}{6}\ e^{j(i)\frac{\pi}{6}}\right) \tag{19}$$

$$T_1 = 3m_a T_s \sin\left(i\frac{\pi}{6} - \omega t\right) \tag{20}$$

$$T_2 = 3m_a T_s \sin\left(\omega t - (i-1)\frac{\pi}{6}\right) \tag{21}$$

$$T_0 = T_S - T_1 - T_2 \tag{22}$$

Coefficients of T_1 and T_2 authenticates that the zero time is reduced subject to the conventional SVM. In each sector, appropriate voltage vectors are applied based on determined dwell-times. Table 2 lists active vectors picked for each sector. Furthermore, calculated switching times for other sectors have been listed in Table 3.

A 13-segment pattern has been selected to apply space vectors to the inverter according to the switching times. The aim is to reduce the switching losses, modify harmonics, and create a symmetrical CMV. Figure 5 illustrates an example of one switching pattern for sector 1, and the CMV in a conventional six-phase inverter, while the SVM is applied. Using vectors V_1 and V_{63} in the switching pattern by considering the goal of better THD and fewer switching loss increases the amplitude of CMV. If other zero vectors are used, this will not result in reduced switching losses. The solution is to reduce the zero switching times. In the proposed SVM, the time of zero vectors (T_0) is reduced. Therefore, the RMS value of CMV and CMC are decreased even with using V_1 and V_{63} as zero vectors.

Table 2. Table of switching vectors in each sector.

Sector	$\boldsymbol{T_1}$	$\boldsymbol{T_2}$
1	(000001),(100011),(110111)	(000011),(100111)
2	(000011),(100111)	(000010),(000111),(101111)
3	(000010),(000111),(101111)	(000110),(001111)
4	(000110),(001111)	(000100),(001110),(011111)
5	(000100),(001110),(011111)	(001100),(011110)
6	(001100),(011110)	(001000),(011100),(111110)
7	(001000),(011100),(111110)	(011000),(111100)
8	(011000),(111100)	(010000),(111000),(111101)
9	(010000),(111000),(111101)	(110000),(111001)
10	(110000),(111001)	(100000),(110001),(111011)
11	(100000),(110001),(111011)	(100001),(110011)
12	(100001),(110011)	(000001),(100011),(110111)

Table 3. Table of switching times in each sector.

Sector 1	Sector 2	Sector 3	Sector 4
$T_{Sa} = T_1 + T_2 + \frac{T_0}{2}$ $T_{Sb} = \frac{2T_1}{3} + T_2 + \frac{T_0}{2}$ $T_{Sc} = \frac{T_1}{3} + \frac{T_2}{2} + \frac{T_0}{2}$ $T_{Sd} = \frac{T_0}{2}$ $T_{Se} = \frac{T_1}{3} + \frac{T_0}{2}$ $T_{Sf} = \frac{2T_1}{3} + \frac{T_2}{2} + \frac{T_0}{2}$	$T_{Sa} = \frac{2T_1}{3} + T_2 + \frac{T_0}{2}$ $T_{Sb} = T_1 + T_2 + \frac{T_0}{2}$ $T_{Sc} = \frac{2T_1}{3} + \frac{T_2}{2} + \frac{T_0}{2}$ $T_{Sd} = \frac{T_1}{3} + \frac{T_0}{2}$ $T_{Se} = \frac{T_0}{2}$ $T_{Sf} = \frac{2T_1}{3} + \frac{T_2}{2} + \frac{T_0}{2}$	$T_{Sa} = \frac{2T_1}{3} + \frac{T_2}{2} + \frac{T_0}{2}$ $T_{Sb} = T_1 + T_2 + \frac{T_0}{2}$ $T_{Sc} = \frac{2T_1}{3} + T_2 + \frac{T_0}{2}$ $T_{Sd} = \frac{T_1}{3} + \frac{T_2}{2} + \frac{T_0}{2}$ $T_{Se} = \frac{T_0}{2}$ $T_{Sf} = \frac{2T_1}{3} + \frac{T_0}{2}$	$T_{Sa} = \frac{T_1}{3} + \frac{T_2}{2} + \frac{T_0}{2}$ $T_{Sb} = \frac{2T_1}{3} + T_2 + \frac{T_0}{2}$ $T_{Sc} = T_1 + T_2 + \frac{T_0}{2}$ $T_{Sd} = \frac{2T_1}{3} + \frac{T_2}{2} + \frac{T_0}{2}$ $T_{Se} = \frac{T_1}{3} + \frac{T_0}{2}$ $T_{Sf} = \frac{T_0}{2}$
Sector 5	Sector 6	Sector 7	Sector 8
$T_{Sa} = \frac{T_1}{3} + \frac{T_0}{2}$ $T_{Sb} = \frac{2T_1}{3} + \frac{T_2}{2} + \frac{T_0}{2}$ $T_{Sc} = T_1 + T_2 + \frac{T_0}{2}$ $T_{Sd} = \frac{2T_1}{3} + T_2 + \frac{T_0}{2}$ $T_{Se} = \frac{T_1}{3} + \frac{T_2}{2} + \frac{T_0}{2}$ $T_{Sf} = \frac{T_0}{2}$	$T_{Sa} = \frac{T_0}{2}$ $T_{Sb} = \frac{T_1}{3} + \frac{T_2}{2} + \frac{T_0}{2}$ $T_{Sc} = \frac{2T_1}{3} + T_2 + \frac{T_0}{2}$ $T_{Sd} = T_1 + T_2 + \frac{T_0}{2}$ $T_{Se} = \frac{2T_1}{3} + \frac{T_2}{2} + \frac{T_0}{2}$ $T_{Sf} = \frac{T_1}{3} + \frac{T_0}{2}$	$T_{Sa} = \frac{T_0}{2}$ $T_{Sb} = \frac{T_1}{3} + \frac{T_0}{2}$ $T_{Sc} = \frac{2T_1}{3} + \frac{T_2}{2} + \frac{T_0}{2}$ $T_{Sd} = T_1 + T_2 + \frac{T_0}{2}$ $T_{Se} = \frac{2T_1}{3} + T_2 + \frac{T_0}{2}$ $T_{Sf} = \frac{T_1}{3} + \frac{T_2}{2} + \frac{T_0}{2}$	$T_{Sa} = \frac{T_1}{3} + \frac{T_0}{2}$ $T_{Sb} = \frac{T_0}{2}$ $T_{Sc} = \frac{T_1}{3} + \frac{T_2}{2} + \frac{T_0}{2}$ $T_{Sd} = \frac{2T_1}{3} + T_2 + \frac{T_0}{2}$ $T_{Se} = T_1 + T_2 + \frac{T_0}{2}$ $T_{Sf} = \frac{2T_1}{3} + \frac{T_2}{2} + \frac{T_0}{2}$
Sector 9	Sector 10	Sector 11	Sector 12
$T_{Sa} = \frac{T_1}{3} + \frac{T_2}{2} + \frac{T_0}{2}$ $T_{Sb} = \frac{T_0}{2}$ $T_{Sc} = \frac{T_1}{3} + \frac{T_0}{2}$ $T_{Sd} = \frac{2T_1}{3} + \frac{T_2}{2} + \frac{T_0}{2}$ $T_{Se} = T_1 + T_2 + \frac{T_0}{2}$ $T_{Sf} = \frac{2T_1}{3} + T_2 + \frac{T_0}{2}$	$T_{Sa} = \frac{2T_1}{3} + \frac{T_2}{2} + \frac{T_0}{2}$ $T_{Sb} = \frac{T_1}{3} + \frac{T_0}{2}$ $T_{Sc} = \frac{T_0}{2}$ $T_{Sd} = \frac{T_1}{3} + \frac{T_2}{2} + \frac{T_0}{2}$ $T_{Se} = \frac{2T_1}{3} + T_2 + \frac{T_0}{2}$ $T_{Sf} = T_1 + T_2 + \frac{T_0}{2}$	$T_{Sa} = \frac{2T_1}{3} + T_2 + \frac{T_0}{2}$ $T_{Sb} = \frac{T_1}{3} + \frac{T_2}{2} + \frac{T_0}{2}$ $T_{Sc} = \frac{T_0}{2}$ $T_{Sd} = \frac{T_1}{3} + \frac{T_0}{2}$ $T_{Se} = \frac{2T_1}{3} + \frac{T_2}{2} + \frac{T_0}{2}$ $T_{Sf} = T_1 + T_2 + \frac{T_0}{2}$	$T_{Sa} = T_1 + T_2 + \frac{T_0}{2}$ $T_{Sb} = \frac{2T_1}{3} + \frac{T_2}{2} + \frac{T_0}{2}$ $T_{Sc} = \frac{T_1}{3} + \frac{T_0}{2}$ $T_{Sd} = \frac{T_0}{2}$ $T_{Se} = \frac{T_1}{3} + \frac{T_2}{2} + \frac{T_0}{2}$ $T_{Sf} = \frac{2T_1}{3} + T_2 + \frac{T_0}{2}$

4. Analysis and results

This section presents experimental results and evaluates those proposed solutions for reducing CMV in six-phase inverters. Results are deduced from a 380 V/5.5 kW prototype. Figure 6 shows the experimental setup and its components. The prototype drive system is connected to a six-phase induction machine, and the machine

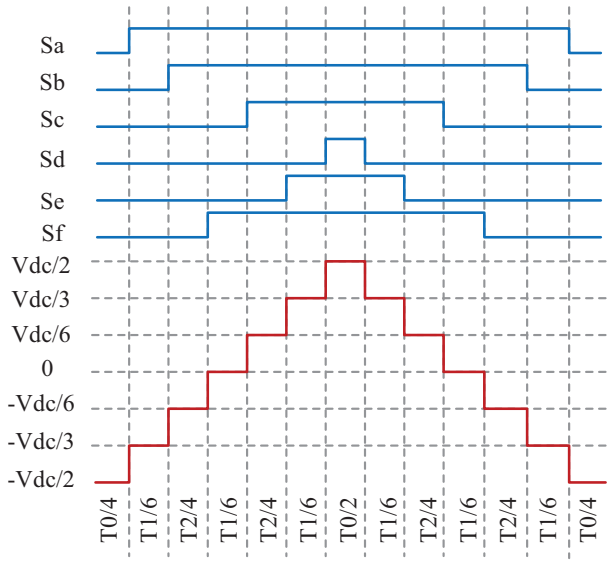

Figure 5. An example of a 13-segment modulation method in sector 1 with the switching pattern, and common mode voltage pattern.

is connected to a rotating mechanical load. This load draws 5.5 kW during its rotation. The TMS320F28335 digital signal processor has executed the modulation strategies on the control board. The gate driver circuit has been designed based on HCPL3120 MOSFET/IGBT drivers. The input DC voltage has been supplied from an autotransformer and a three-phase bridge rectifier with a bulky capacitor. The GW-INSTEK GDS-2074 Oscilloscope captures experimental results. Table 4 summarizes the specifications of the experimental prototype. Three test cases are designed, which are expressed in the following.

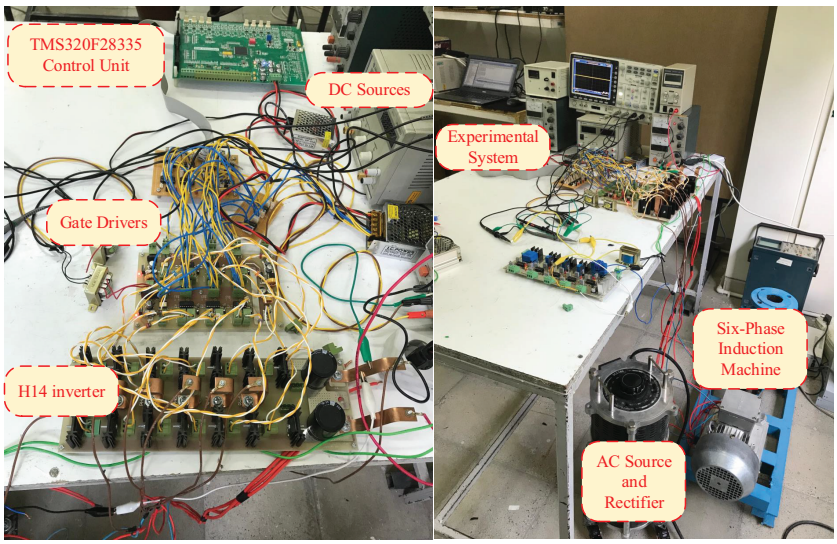

Figure 6. Figures of experimental set-up.

Table 4. Experimental prototype and motor specifications.

Parameters	Value	Parameters	Value
Input DC voltage	550V	Output frequency	50Hz
Output line-line RMS voltage	380V	Output power	5.5kW
Base switching frequency	5 kHz	Current sensor	LEM-LA55
Gate drivers	HCPL3120	Power IGBTs	BUP314D
Modulation index	0.64	Rated speed	1500rpm
Poles	4	Load type	$T = k\omega$
Nominal torque	35 N.m		

4.1. Analysis of the proposed six-phase inverter

In this test, the performance of the modified topology is evaluated. The SPWM strategy is applied. The selected switching frequency is 5 kHz. As stated before, in this topology, the inverter is disconnected from the input source when switching events 0 or 63 are applied. Figures 7a–7c represent the experimental results of this test. In Figure 7a, the line-line voltages are presented. Figure 7b illustrates the current waveform of each phase. These results confirm the operation of this topology in terms of the output voltage, the output current, and the phase differences. Figure 7c depicts CMV and CMC. CMC is reduced to 75% below the standard value. Figures 8a and 8b display the power losses distribution of this modified six-phase inverter. In the hardware method, only two power switches are added to the classical topology. From Figures 8a and 8b, each of them produces 38% and 44% of the total switching and conduction losses of the converter. Thus, if they do not exist, these two losses are eliminated.

4.2. Analysis of the proposed six-phase space vector modulation

SVM decreases the CMV and CMC due to providing two features. The first feature corresponds to the modulation pattern. By considering twelve sectors, zero vector times are divided into three times. Also, the modulation pattern is symmetrical. The second feature is the ability to optimize the zero vector times by the coefficients of Equation (18). By reducing the zero vector times, the common mode is diminished. This section evaluates the performance of the proposed SVM on the CMV and CMC. This modulation strategy is applied to a conventional six-phase bridge inverter. The switching frequency is set to 5 kHz. Figure 9 represents the result of the common mode analysis. Results indicate that the proposed modulation strategy can reduce the common mode current to 45% below the standard value. The common mode is reduced further by choosing higher switching frequencies. It is happened due to the significant reduction of application times of zero vectors in each switching interval. In order to show this feature, the proposed modulation strategy is implemented with different switching frequencies. Figures 10a and 10b show the results of this test. Operating with 15kHz switching frequency helps decrease the value of common mode current to 86% below the standard.

4.3. The effect of proposed SVM on machine speed and torque

In this section, the effect of the proposed SVM on the machine speed and torque is represented. In order to capture wide data from torque and speed, a data acquisition module (OWON VDS-1022I) is used. The results are displayed by MATLAB software. The load torque is varied by speed, as mentioned in Table 4. Voltage-frequency constant algorithm is employed. The acceleration and deceleration times are adjusted at 7 s. The

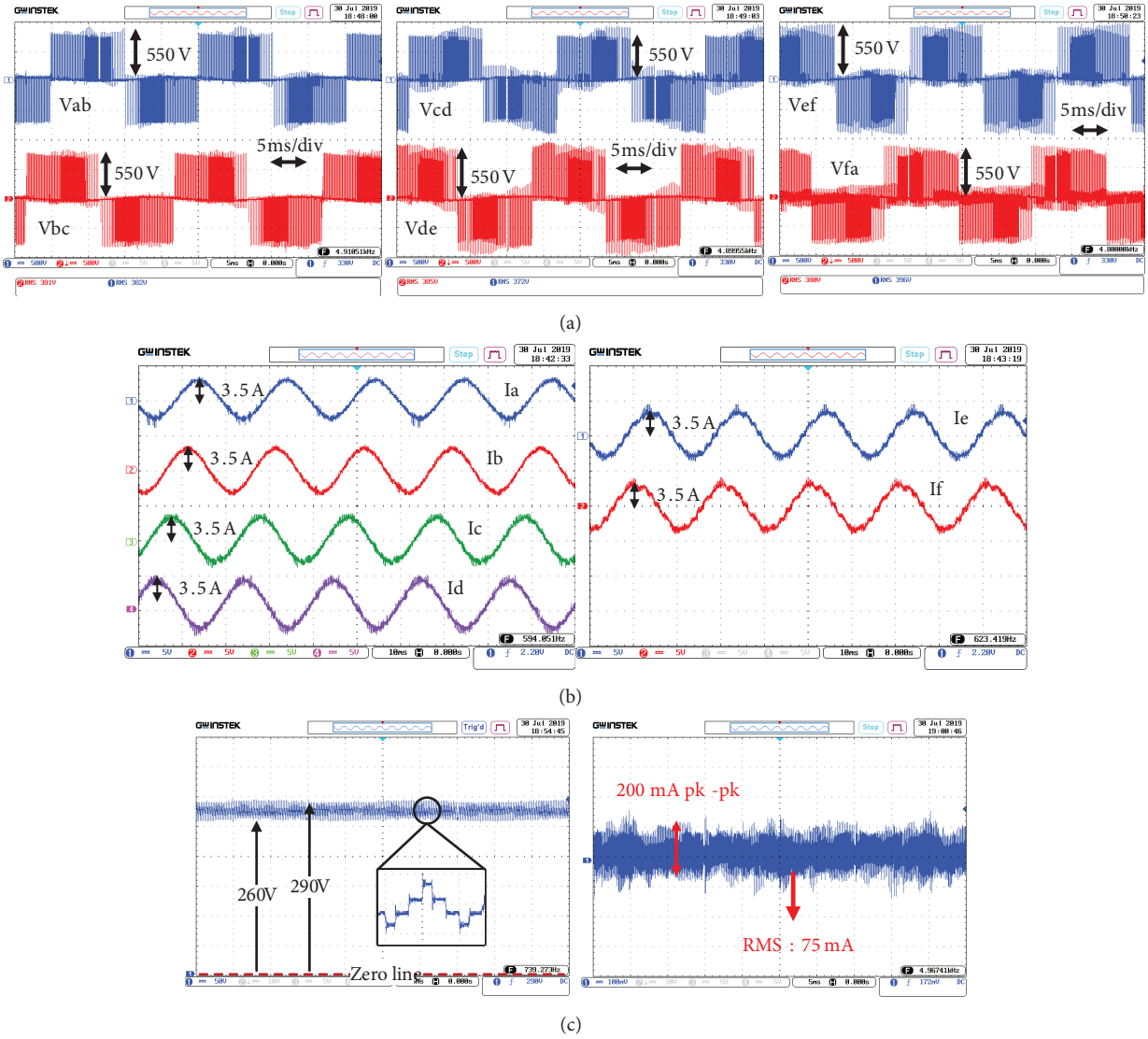

Figure 7. Key experimental result of the proposed topology, (a) V_{ab} and V_{bc}, V_{cd}, V_{de}, V_{ef} and V_{fa}, (b) phase currents a to f, (c) common mode voltage and current.

reference speed is changed, according to Figure 11. In the startup stage, to reduce the startup current, a V/F curve is employed. The startup current is two times greater than the nominal current. Figure 11 confirms that the proposed SVM does not reduce the control quality. This paper does not investigate the drive control system. Actually, using modern control techniques like predictive control improves the dynamic response of the machine.

4.4. Discussion

To analyze the above achievements, common mode values have been measured for three possible designs. Table 5 organizes all results to compare them. Accordingly, the conventional inverter with SPWM cannot satisfy the CMC standard. Also, the output current THD is higher than the standard value (5%) in this type of

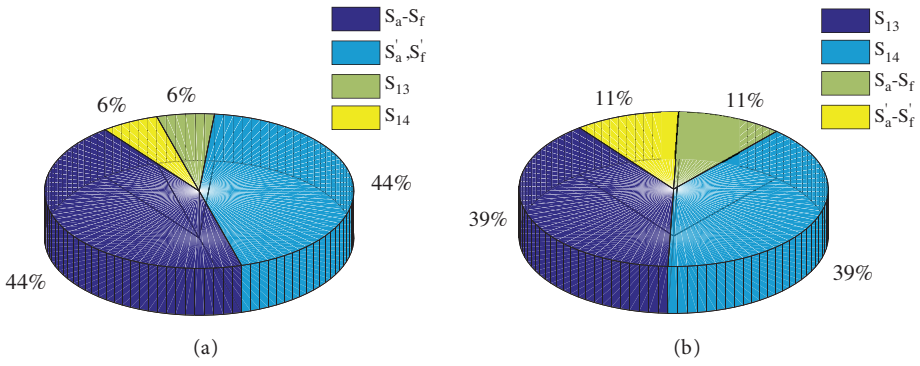

Figure 8. Distribution of power losses in H14 inverter, (a) switching losses, (b) conduction losses.

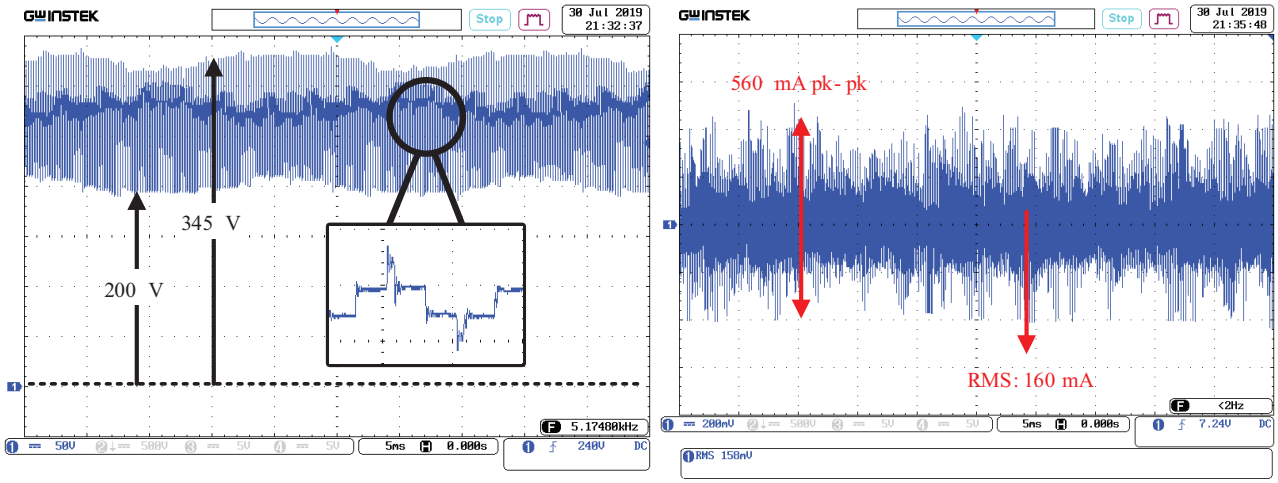

Figure 9. The value of common mode voltage and current under applying the proposed space vector modulation.

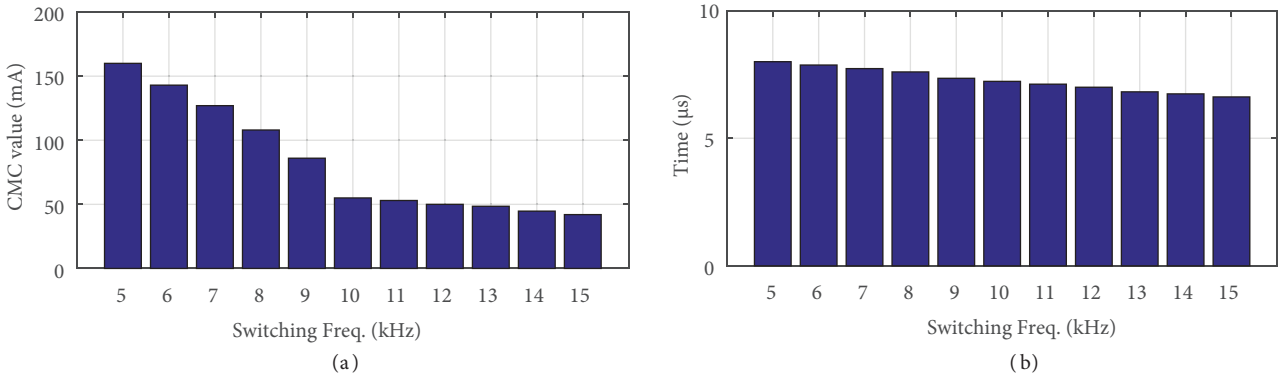

Figure 10. Common mode for different switching frequencies, (a) common mode value, (b) zero vector switching times.

inverter and modulation method. The conventional inverter with SVM satisfies CMC's standard requirement because it reduces the CMC to 160mA, which is 45% lower than the standard value. Furthermore, due to using a symmetrical switching pattern, it provides standard output current THD. The modified six-phase inverter

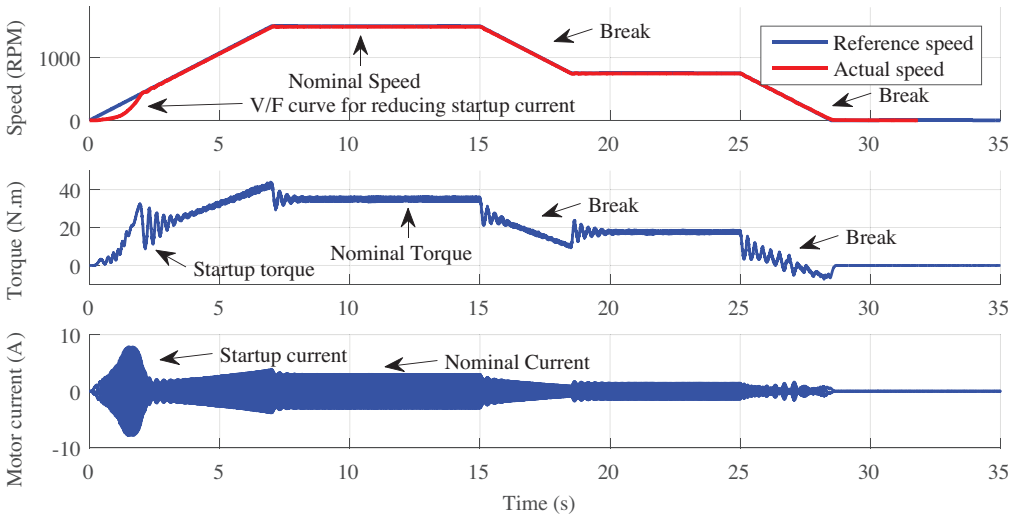

Figure 11. Experimental results of torque and speed under the proposed SVM.

reduces the CMC remarkably. So, it performs better common mode characteristics due to suppressing the maximum value of common mode voltage. As shown in Table 5, the current THD of the proposed modified inverter is also higher than the standard value due to SPWM. Although the modulation method decreases the CMC in other literature, the current THD is still higher than the IEEE 519 standard. Efficiency is another critical parameter. Classical six-phase inverters provide good efficiency that is around 97.3%. The recommended modified topology includes two additional power switches. According to results, by adding these power switches, efficiency is reduced to 96.7%, which does not experience a significant change. The proposed modulation has a larger amplitude modulation index than other previous modulation methods proposed for six-phase inverter because the number of sectors is twice the conventional SPWM method for six-phase inverters. Besides, according to the output current data and the FFT analysis in MATLAB software (as shown in Table 5), the proposed SVM provides 4.35% THD in output current, as illustrated by Figure 12, which is lower than IEEE519 standard (5%) and other literature in Table 5.

Table 5. Comparison between methods.

Topology	Modulation	CMC	Reduction value	Current THD
Proposed inverter	SPWM	75 mA	75% below	5.53%
Conventional inverter	SPWM	706 mA	133% above	5.53%
Conventional inverter	Proposed SVM	160 mA	45% below	4.35%
Method in [8]	SVM	100 mA	67% below	6.13%
Phase-shifted SPWM-1 in [16]	SPWM	231 mA	33% below	7.19%
Sawtooth carrier-based SPWM in [15]	SPWM	100 mA	67% below	6.93%
Modulation method in [17]	SVM	234 mA	20% below	8.48%

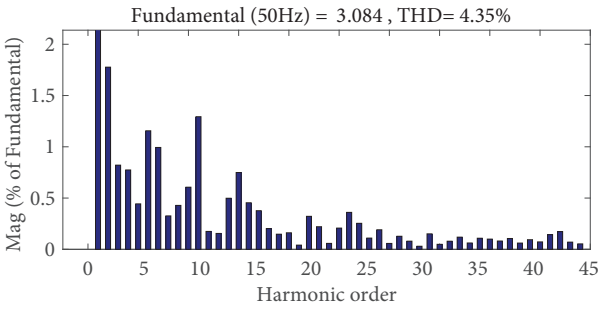

Figure 12. Output current THD with the proposed SVM.

References

[1] Levi E, Bojoi R, Toliyat HA, Williamson S. Multiphase induction motor drives - a technology status review. IET Electric Power Applications 2007; 1 (4): 489-516.

[2] Chen H, Zhao H. Review on pulse-width modulation strategies for common-mode voltage reduction in three-phase voltage-source inverters. IET Power Electronics 2016; 9 (14): 2611-2620.

[3] Adabi J, Boora AA, Zare F, Nami A, Ghosh A et al. Common-mode voltage reduction in a motor drive system with a power factor correction. IET Power Electronics 2012; 5 (3): 366-375.

[4] Adabi J, Zare F, Ledwich G, Ghosh A. Leakage current and common mode voltage issues in modern ac drive systems. In: Australasian Universities Power Engineering Conference; Perth, Australia; 2007. pp. 1-6.

[5] Rahimi R, Farhangi S, Farhangi B, Moradi GR, Afshari E et al. H8 inverter to reduce leakage current in transformerless three-phase grid-connected photovoltaic systems. IEEE Journal of Emerging and Selected Topics in Power Electronics 2018; 6(2): 910-918.

[6] Barater D, Franceschini G, Immovilli F, Lorenzani E. Investigation on h-8 vsi architecture for bearing currents mitigation in vfd. In: 43rd Annual Conference of the IEEE Industrial Electronics Society (IECON); Beijing, China; 2017. pp. 4391–4396.

[7] Concari L, Barater D, Buticchi G, Concari C, Liserre M. H8 inverter for common-mode voltage reduction in electric drives. IEEE Transactions on Industry Applications 2016; 52 (5): 4010-4019.

[8] Zheng J, Rong F, Li P, Huan S, He Y. Six-phase svpwm with common-mode voltage suppression. IET Power Electronics 2018; 11 (15): 2461-2469.

[9] Pandit JK, Aware MV, Nemade R, Tatte Y. Simplified implementation of synthetic vectors for dtc of asymmetric six-phase induction motor drives. IEEE Transactions on Industry Applications 2018; 54 (3): 2306-2318.

[10] Shang J, Li W, Zargari R, Cheng Z. Pwm strategies for common-mode voltage reduction in current source drives. IEEE Transactions on Power Electronics 2014; 29 (10): 5431-5445.

[11] Hou C, Shih C, Cheng P, Hava AM. Common-mode voltage reduction pulsewidth modulation techniques for three-phase grid-connected converters. IEEE Transactions on Power Electronics 2013; 28 (4): 1971-1979.

[12] Marouani K, Baghli L, Hadiouche D, Kheloui A, Rezzoug A. A new pwm strategy based on a 24-sector vector space decomposition for a six-phase vsi-fed dual stator induction motor. IEEE Transactions on Industrial Electronics 2008; 55 (5): 1910-1920.

[13] Lee S, Jung J, Hwnag S, Kim J, Cho H. Common mode voltage reduction method for h7 inverter using dpwm offset based modulation technique. In: IEEE Energy Conversion Congress and Exposition (ECCE); Portland, USA; 2018. pp. 1790-1795.

[14] Guo X. Three-phase ch7 inverter with a new space vector modulation to reduce leakage current for transformerless photovoltaic systems. IEEE Journal of Emerging and Selected Topics in Power Electronics 2017; 5 (2): 708-712.

[15] Liu Z, Zheng Z, Peng Z, Li Y, Hao L. A sawtooth carrier-based pwm for asymmetrical six-phase inverters with improved common-mode voltage performance. IEEE Transactions on Power Electronics 2018; 33 (11): 9444-9458.

[16] Liu Z, Zheng Z, Sudhoff D, Gu C, Li Y. Reduction of common-mode voltage in multiphase two-level inverters using spwm with phase-shifted carriers. IEEE Transactions on Power Electronics 2018; 31 (9): 6631-6645.

[17] Pulvirenti M, Scarcella G, Scelba G, Cacciato M. Space vector modulation technique for common mode currents reduction in six phase ac drives. In: 15th European Conference on Power Electronics and Applications(EPE); Lile, France; 2013. pp. 1-10.

[18] Guzinski J. Common-Mode Voltage and Bearing Currents. In: Rathnayake D (editor). PWM Inverters: Causes, Effects and Prevention. USA: John Wiley & Sons, Ltd, 2014, pp. 664-694.

[19] Wang Y, Liu W, Chen Z, Bai B. Calculation of high frequency bearing currents of pwm inverter-fed vf induction motor. In: International Power Electronics and Application Conference and Exposition; Shanghai, China; 2014. pp. 1428-1433.

[20] Magdun O, Binder A. High-frequency induction machine modeling for common mode current and bearing voltage calculation. IEEE Transactions on Industry Applications 2014; 50 (3): 1780-1790.